Structure of the Self-Consistent Solutions for Even-Even Nuclei in the $2p$-$1f$ Shell*

J. C. PARIKH
Department of Physics and Astronomy, University of Rochester, Rochester, New York 14627
AND
J. P. SVENNE
The Niels Bohr Institute, University of Copenhagen, Copenhagen, Denmark
(Received 19 June 1968)

Results of Hartree-Fock calculations on even-even nuclei in the $2p$-$1f$ shell are presented. The method of Kelson and Levinson is used, whereby Ca^{40} is taken as an inert core and the Hartree-Fock variation is done only on the particles outside Ca^{40} moving in the $2p$-$1f$ shell. Binding energies, 2^λ-pole moments, and single-particle structure of a number of nuclei are calculated. The total pickup strengths for neutrons and protons are calculated. It is found that, as in the $2s$-$1d$ shell, the SU_3 scheme is quite good and only weakly broken by the spin-orbit force. However, the gap between occupied and unoccupied levels is smaller by a factor of 3 than in the s-d shell. Therefore, particle-hole excitations and correlation effects have a much stronger influence on the low-energy structure of the p-f-shell nuclei.

INTRODUCTION

In recent years, a considerable number of Hartree-Fock (HF) calculations have been carried out in the $2s$-$1d$ shell. In most of these, the method of Kelson and Levinson[1] has been used, whereby an inert core is assumed and the variation implied in the HF method is only over the relatively few "valence" nucleons. In the case of s-d-shell nuclei, O^{16} is a suitable core and all the valence particles are confined to the $2s$-$1d$ shell. Empirically, the nuclei of the s-d shell show clearly deformed structures which can be found to arise from deformed self-consistent fields.[2]

The considerable success of the HF calculations in the s-d shell has encouraged extending such calculations to other regions, in particular the $2p$-$1f$ shell. The nuclei in the beginning of the p-f shell do not show the characteristic deformed structure of the s-d-shell nuclei. It has been suggested[3] that this may be due to the competition between the spin-orbit force with the field-producing forces leading to a Q_{20}-type deformation. It was therefore decided to carry out HF calculations of the Kelson-Levinson type for even-even nuclei of the $2p$-$1f$ shell. In this case, the inert core is taken as Ca^{40} and the HF variation is done over the extra particles moving in the $2p$-$1f$ shell.

Also of interest was to see if parallels could be found between nuclei of the s-d and f-p shells; for example, does Ti^{44} in any way resemble Ne^{20}, both of which have two protons and two neutrons outside the core. Another question was whether multiple solutions, such as those found[4] in Ne^{20} and Mg^{24}, can also be found in the p-f shell.

I. METHOD OF CALCULATION

A. HF Equations

In the HF method,[1] the intrinsic ground state of the nucleus is considered to be a single determinant of single-particle states $|\lambda\rangle$ which are eigenstates of the HF Hamiltonian

$$\langle j_1 m_1|h|j_2 m_2\rangle = e_{j_1}\delta_{j_1 j_2} + \sum_{\lambda=1}^{N}\langle j_1 m_1, \lambda|v|j_2 m_2, \lambda\rangle_A . \quad (1)$$

Here, e_j are single-particle energies appropriate to the nucleus chosen as the inert core and are taken from experiment (see Table I). N is the number of particles outside the core, and λ are the occupied HF orbitals. The subscript A on the matrix element of the two-body potential v denotes antisymmetrization. The HF orbitals $|\lambda\rangle$ are expanded in a basis $|jm\rangle$ of eigenstates, in the $2p$-$1f$ shell, of the spherical harmonic oscillator

$$|\lambda\rangle = \sum C_{jm}{}^{\lambda}|jm\rangle . \quad (2)$$

To obtain axially symmetric solutions, the summation here is on j only. If the summation runs over m also, triaxial solutions can be obtained.

The HF equations are Eq. (1) together with the eigenvalue problem:

$$h|\lambda\rangle = \epsilon_\lambda|\lambda\rangle . \quad (3)$$

TABLE I. The single-particle energies, in MeV, used in Eq. (1).

j	Proton	Neutron
$f_{7/2}$	−1.09	−8.36
$p_{3/2}$	0.70	−6.29
$f_{5/2}$	4.41	−2.86
$p_{1/2}$	3.04	−4.23

* This work was supported in part by the U. S. Atomic Energy Commission (J. C. P.), the National Research Council, Canada, and the Canadian-Scandinavian Foundation (J.P.S.). The computations were carried out at the Northern European Computation Center, Danmarks Tekniske Hojskole.

[1] I. Kelson, Phys. Rev. **132**, 2189 (1963); I. Kelson and C. A. Levinson, *ibid.* **134**, B269 (1964).

[2] J. Bar-Touv and I. Kelson, Phys. Rev. **138**, B1035 (1965).

[3] K. H. Bhatt and J. C. Parikh, Phys. Letters **24B**, 613 (1967).

[4] J. C. Parikh, Phys. Letters **25B**, 181 (1967).

TABLE II. Calculated properties of the even-even nuclei with the Yale-Shakin interaction. Under "type," A stands for axial, T for triaxial solutions. E_{HF} are the calculated HF energies [Eq. (4)], $(BE)_{expt}$ are the experimental binding energies (see Ref. 10), relative to Ca^{40}. All energies are given in MeV. The $Q_{\lambda 0}$ moments are given in units of b^{λ}, where $b=2.09$ fm is the oscillator radius used. G_p and G_n are the proton and neutron gaps, respectively. The intrinsic quadrupole moment is $\epsilon=2Q_{20}$.

Nucleus	Type	$-E_{HF}$	$(BE)_{expt}$	Q_{20}	Q_{40}	Q_{60}	G_p	G_n
Ca^{42}	A	17.168	19.835	−3.00	4.50	−3.75		0.005
	A	17.113		2.61	7.80	25.66		0.06
Ca^{44}	T	35.130	38.898	3.92	4.11	−4.70		0.20
	A	35.104		4.48	5.92	−18.01		0.10
Ca^{46}	A	53.581	56.719	3.94	−5.52	4.00		0.20
Ca^{48}	sph.	72.568	73.940	0	0	0		1.94
Ti^{44}	A	25.322	33.531	9.82	34.05	89.98	2.38	2.34
	A	23.594		−6.00	9.00	−7.5	0.53	0.53
Ti^{46}	A	46.115	56.139	12.23	31.75	43.22	2.19	0.88
	A	44.167		−7.21	4.57	4.38	0.88	0.36
Ti^{48}	A	65.926	76.642	11.52	21.67	73.81	1.86	0.49
	A	64.470		−7.78	8.28	−25.13	0.94	0.02
	A	85.597		14.86	18.35	17.97	1.53	0.30
Ti^{50}	T	85.366	95.733	3.77	4.36	−50.68	1.36	1.36
	A	85.289		−7.77	17.11	−23.57	1.07	1.32
	T	56.543		15.85	28.13	−17.35	2.24	2.24
Cr^{48}	A	55.876	69.664	15.26	28.00	−12.41	1.15	1.17
	A	52.687		−8.66	1.30	14.22	0.43	0.46
Cr^{50}	A	79.009	92.986	18.81	24.23	75.72	2.00	0.43
	A	75.329		−10.43	9.68	−18.82	0.36	0.20
Cr^{52}	A	102.198	114.291	18.65	13.83	−51.30	1.74	1.27
	A	99.043		−14.56	35.03	−69.05	0.32	2.36
Cr^{54}	A	123.846	131.953	14.93	21.62	−54.82	1.61	0.98
	A	120.952		−11.63	9.34	−0.26	0.60	0.49
	A	90.899		22.33	19.71	−129.75	0.70	0.67
Fe^{52}	A	87.004	105.643	−14.81	27.32	−53.90	0.27	0.22
	A	86.704		−16.18	43.42	−78.01	0.44	0.37
Fe^{54}	A	116.790	129.704	22.51	10.15	−104.01	0.41	1.92
	A	114.488		−18.65	44.90	−78.27	0.14	2.95
	T	139.975		18.35	18.89	−91.67	0.39	0.77
Fe^{56}	A	138.385	150.206	−16.96	27.72	−53.44	0.49	0.35
	A	137.152		7.54	−37.14	−86.32	1.73	0.67
Fe^{58}	A	162.789	167.890	−16.80	16.14	−32.78	0.42	0.23
Ni^{56}	A	131.440	141.954	22.60	0.23	−74.79	2.46	2.53
	A	131.202		−21.35	48.27	−82.01	3.28	3.28
	T	157.649		22.64	−13.47	37.02	1.55	0.78
Ni^{58}	A	157.025	164.406	−20.84	38.48	−65.47	2.83	0.26
	A	156.972		22.55	−13.52	−30.87	1.58	0.38
Ni^{60}	T(?)	183.897	184.792	19.62	−5.46	−42.59	0.97	1.15
Ni^{62}	A	210.827	203.213	−19.72	20.16	23.02	1.89	2.51
	A	210.407		19.37	−20.27	−5.75	1.16	2.12
Zn^{62}	A	201.115	196.431	−20.06	17.64	−24.70	0.34	0.50
Zn^{64}	A	230.637	217.117	20.14	−29.65	32.24	0.60	2.31
Zn^{68}	A	286.543	253.194	−11.41	−17.92	−11.58	0.45	2.51
	A	285.529		8.22	−0.68	−8.90	0.77	0.81
Ge^{64}	A	219.166		−20.68	7.16	5.18	0.53	0.43
Ge^{70}	A	311.35	268.502	−11.84	−21.46	1.21	0.02	2.64
Ge^{72}	sph.	342.099	286.885	0	0	0	1.16	

Since h itself depends on its eigenvectors $|\lambda\rangle$, the problem must be solved self-consistently by an iterative method. One starts with a guess for $|\lambda\rangle$, calculates h, diagonalizes to get a new set of $|\lambda\rangle$, and so on, until the total energy

$$E_{HF}=\tfrac{1}{2}\sum_{\lambda\lambda'}[e_j C_{jm}{}^{\lambda} C_{jm}{}^{\lambda'}+\epsilon_\lambda \delta_{\lambda\lambda'}] \quad (4)$$

converges to a constant value. It is possible that different starting wave functions $|\lambda\rangle$ lead to quite different structures of the final solution.[4]

B. Two-Body Potential

Most HF calculations in the s-d shell[2,4] have used the Rosenfeld force.[5] However, this force is not suitable for the p-f shell. In this work, we have used the effective interaction derived by Shakin *et al.*[6] from the Yale[7] potential.[8] The Yale potential is a "realistic" one in the sense that it fits the nucleon-nucleon scattering data, and it has a hard core. Shakin *et al.*[6] have calculated a nonsingular reaction matrix from this potential, including the dominant second-order term due to the tensor force. They provide a list of matrix elements of

[5] L. Rosenfeld, *Nuclear Forces* (North-Holland Publishing Co., Amsterdam, 1948), p. 233.

[6] C. M. Shakin, Y. R. Waghmare, and M. H. Hull, Jr., Phys. Rev. **161**, 1006 (1967); C. M. Shakin, Y. R. Waghmare, M. Tomaselli, and M. H. Hull, Jr., *ibid.* **161**, 1015 (1967).

[7] K. E. Lassila, M. H. Hull, Jr., H. M. Ruppel, F. A. McDonald, and G. Breit, Phys. Rev. **126**, 881 (1962).

[8] In the s-d shell, the structure of the solutions obtained with this potential does not differ significantly from that due to the Rosenfeld force (see Ref. 4); therefore comparisons between s-d shell and p-f shell results can still be made.

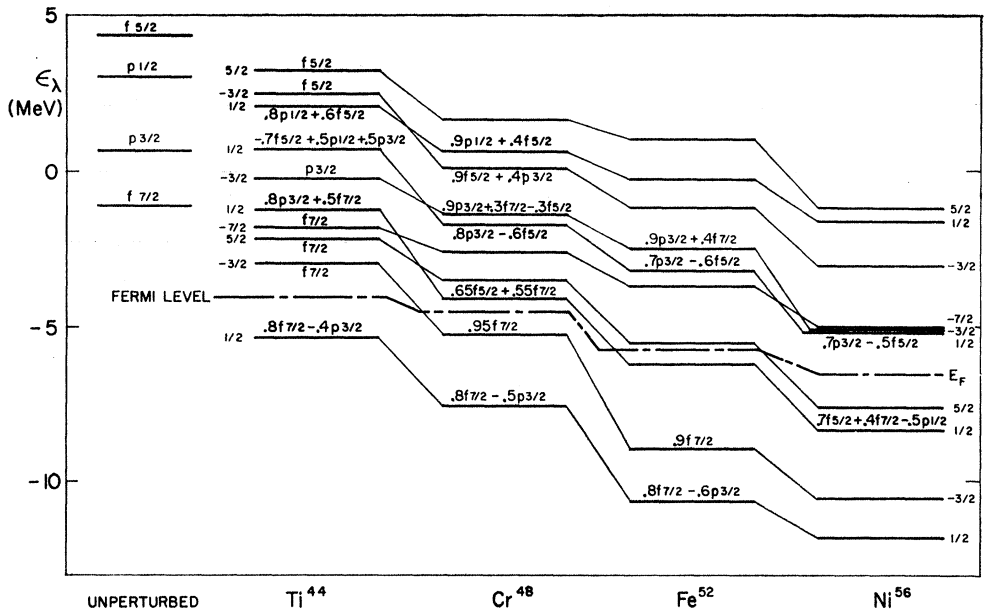

FIG. 1. Proton single-particle HF levels for the prolate, axial solutions of $N=Z$ nuclei. The "unperturbed" levels are the single-particle energies e_{kj} listed in Table I. The levels are labeled by the value of k and on each level are given the dominant terms in their oscillator expansion [Eq. (2)]. The thin lines connect levels of the same k and approximately same structure. Significant changes in structure of the levels from one nucleus to the next are indicated.

this reaction matrix in relative coordinates, from which the two-body matrix elements required in Eq. (1) may be calculated. We have used the matrix elements for oscillator radius $b=[\hbar/(M\omega)]^{1/2}=2.09$ fm, which is appropriate for this region.

As a simplified model to help understand the nature of the deformed HF solutions in the *s-d* shell, Bar-Touv and Levinson[9] have considered an infinite-range force with the same exchange mixture as the finite-range one. This provides a "zero-order scheme" for the HF solutions as an aid in explaining the finite-range results. Because the Yale-Shakin potential arises out of a rather complicated calculation, its infinite-range limit is not easily taken. We have therefore chosen a rather crude model interaction for the infinite-range potential (see the Appendix).

$$V_\infty=-V_0(W+MP_x+BP_\sigma-HP_\tau), \qquad (5)$$

with $V_0=2.57$ MeV, $W=0.245$, $M=0.913$, $B=-0.365$, $H=-0.206$. Though this is a rough approximation of the exchange mixture, we hope that it is good enough to give the gross structure of the solutions.

II. RESULTS OF FINITE-RANGE CALCULATION

The results of the HF calculation with the Yale-Shakin potential are given in Tables II and III. Table II gives the HF energies, relative to the Ca^{40} binding energy, compared with the experimental energies.[10] Also listed are expectation values of Q_{20}, Q_{40}, and Q_{60}, where

$$Q_{\lambda\mu}=\left(\frac{4\pi}{2\lambda+1}\right)^{1/2}\left(\frac{r}{b}\right)^\lambda Y_{\lambda\mu}(\Omega), \qquad (6)$$

and the gaps[9] between occupied and unoccupied levels. An examination of these results shows that the lowest-energy solution for most of these nuclei is axial and prolate. A few examples of triaxial lowest solutions were found, namely Cr^{48}, Fe^{56}, and Ni^{58}. Cases of oblate lowest solutions are seen only among the heaviest nuclei[11] studied here, namely Zn^{68}, Ge^{64}, and Ge^{70} (only oblate solutions were found for the latter two). There does not appear to be such a richness of solutions as seen[4] in Ne^{20} and Mg^{24}. In only one case, Fe^{52}, were there two oblate solutions, and both are more than 3 MeV above the prolate ground state.

The agreement of the calculated binding energies with the experimental ones is quite good. They are generally too low, except for the heaviest nuclei. This is good, because the HF method is based on a variational principle. Therefore, any improvement of the wave function, such as by increasing the basis space, would tend to increase the binding. Another source of discrepancy might be inadequacies in the effective two-body interaction used. Finally, the overbinding of the heaviest nuclei is likely due to the neglect of all effects of the Coulomb force other than the shift between the proton and neutron single-particle energies (see Table I). If the Coulomb potential were included in the

[9] J. Bar-Touv and C. A. Levinson, Phys. Rev. **153**, 1099 (1967).
[10] L. A. König, J. H. E. Mattauch, and A. H. Wapstra, Nucl. Phys. **31**, 18 (1962).
[11] The lowest-energy solution in Ca^{42} is also oblate, but it is nearly degenerate with the prolate one.

TABLE III. The HF single-particle orbitals (Yale-Shakin interaction). $\epsilon_k(\epsilon_\lambda)$ are the single-particle energies in MeV. In the columns labeled $f_{7/2,k}$, $p_{3/2,k}$, etc., are given the expansion coefficients C_{jk}^{λ} of the single-particle orbitals [Eq. (2)]. Orbitals above the solid line are occupied, the ones below unoccupied. In parts (k), (l), and (m), the triaxial cases, the coefficients are listed in the order $f_{7/2,1/2}$, $p_{3/2,1/2}$, $f_{5/2,1/2}$, $p_{1/2,1/2}$, $f_{7/2,-3/2}$, $p_{3/2,-3/2}$, $f_{5/2,-3/2}$, $f_{7/2,5/2}$, $f_{5/2,5/2}$, $f_{7/2,-7/2}$.

(a) Ca^{42}, axial, oblate.

Protons						Neutrons					
ϵ_k	k	$f_{7/2,k}$	$P_{3/2,k}$	$f_{5/2,k}$	$P_{1/2,k}$	ϵ_k	k	$f_{7/2,k}$	$P_{3/2,k}$	$f_{5/2,k}$	$P_{1/2,k}$
−2.989	$-\frac{7}{2}$	1.0	···	···	···	−8.808	$-\frac{7}{2}$	1.0	···	···	···
−2.294	$\frac{5}{2}$	0.991	···	0.136	···						
−2.002	$-\frac{3}{2}$	−0.975	−0.224	0.013	···	−8.803	$\frac{5}{2}$	0.996	···	0.087	···
−1.889	$\frac{1}{2}$	0.982	0.179	0.014	0.058	−8.674	$-\frac{3}{2}$	−0.997	−0.065	0.030	···
−0.395	$-\frac{3}{2}$	−0.222	0.971	0.084	···	−8.637	$\frac{1}{2}$	0.997	0.069	0.008	0.021
0.064	$\frac{1}{2}$	−0.186	0.967	0.019	0.172	−6.756	$-\frac{3}{2}$	−0.065	0.998	0.021	···
1.825	$\frac{5}{2}$	0.136	···	−0.991	···	−6.595	$\frac{1}{2}$	0.071	−0.994	0.007	−0.086
1.976	$\frac{1}{2}$	0.027	0.178	−0.297	−0.938	−4.778	$\frac{1}{2}$	0.015	0.087	−0.033	−0.996
2.891	$-\frac{3}{2}$	0.032	−0.079	0.996	···	−4.135	$\frac{5}{2}$	0.087	···	−0.996	···
3.217	$\frac{1}{2}$	−0.002	0.033	0.955	−0.296	−3.702	$-\frac{3}{2}$	0.031	−0.019	0.999	···
						−3.534	$\frac{1}{2}$	0.008	−0.009	−0.999	0.032

(b) Ca^{42}, axial, prolate.

Protons						Neutrons					
ϵ_k	k	$f_{7/2,k}$	$P_{3/2,k}$	$f_{5/2,k}$	$P_{1/2,k}$	ϵ_k	k	$f_{7/2,k}$	$P_{3/2,k}$	$f_{5/2,k}$	$P_{1/2,k}$
−2.994	$\frac{1}{2}$	0.971	−0.191	−0.125	0.071	−8.785	$\frac{1}{2}$	0.995	−0.076	−0.055	0.031
−2.390	$-\frac{3}{2}$	0.997	−0.058	0.059	···						
−1.993	$\frac{5}{2}$	−1.000	···	0.022	···	−8.841	$-\frac{3}{2}$	0.998	−0.030	0.049	···
−1.770	$-\frac{7}{2}$	1.0	···	···	···	−8.685	$\frac{5}{2}$	−1.000	···	0.023	···
−0.394	$\frac{1}{2}$	−0.211	−0.966	−0.095	0.116	−8.605	$-\frac{7}{2}$	1.0	···	···	···
0.026	$-\frac{3}{2}$	0.060	0.997	−0.044	···	−6.760	$\frac{1}{2}$	−0.079	−0.995	−0.021	0.065
1.724	$\frac{1}{2}$	−0.107	0.174	−0.722	0.661	−6.597	$-\frac{3}{2}$	0.031	0.999	−0.019	···
2.342	$\frac{1}{2}$	0.036	0.015	0.673	0.738	−4.789	$\frac{1}{2}$	−0.031	0.069	−0.099	0.992
2.710	$-\frac{3}{2}$	0.056	−0.047	−0.997	···	−4.062	$\frac{1}{2}$	0.050	−0.018	0.993	0.102
3.152	$\frac{5}{2}$	0.022	···	1.000	···	−3.784	$-\frac{3}{2}$	0.044	−0.021	−0.999	···
						−3.511	$\frac{5}{2}$	0.023	···	1.000	···

(c) Ti^{44}, axial, prolate.

Protons						Neutrons					
ϵ_k	k	$f_{7/2,k}$	$P_{3/2,k}$	$f_{5/2,k}$	$P_{1/2,k}$	ϵ_k	k	$f_{7/2,k}$	$P_{3/2,k}$	$f_{5/2,k}$	$P_{1/2,k}$
−5.316	$\frac{1}{2}$	0.830	−0.425	−0.295	0.210	−12.546	$\frac{1}{2}$	0.838	−0.407	−0.295	0.211
−2.932	$-\frac{3}{2}$	0.986	−0.127	0.109	···	−10.201	$-\frac{3}{2}$	0.987	−0.117	0.109	···
−2.113	$\frac{5}{2}$	−0.999	···	0.035	···	−9.377	$\frac{5}{2}$	−0.999	···	0.035	···
−1.749	$-\frac{7}{2}$	1.0	···	···	···	−9.011	$-\frac{7}{2}$	1.0	···	···	···
−1.204	$\frac{1}{2}$	−0.540	−0.771	−0.241	0.236	−8.318	$\frac{1}{2}$	−0.533	−0.749	−0.285	0.272
−0.198	$-\frac{3}{2}$	0.137	0.986	−0.094	···	−7.195	$-\frac{3}{2}$	0.128	0.986	−0.107	···
0.734	$\frac{1}{2}$	−0.137	0.473	−0.704	0.512	−6.471	$\frac{1}{2}$	−0.113	0.521	−0.686	0.495
2.133	$\frac{1}{2}$	0.030	0.036	0.600	0.799	−5.136	$\frac{1}{2}$	0.030	0.040	0.601	0.798
2.526	$-\frac{3}{2}$	0.096	−0.107	−0.990	···	−4.735	$-\frac{3}{2}$	0.095	−0.120	−0.988	···
3.302	$\frac{5}{2}$	0.035	···	0.999	···	−3.958	$\frac{5}{2}$	0.035	···	0.999	···

(d) Ca^{48}, spherical.

Protons						Neutrons					
ϵ_k	k	$f_{7/2,k}$	$P_{3/2,k}$	$f_{5/2,k}$	$P_{1/2,k}$	ϵ_k	k	$f_{7/2,k}$	$P_{3/2,k}$	$f_{5/2,k}$	$P_{1/2,k}$
−5.673	$\frac{1}{2}$	1.0	0.0	0.0	0.0	−9.782	$\frac{1}{2}$	1.0	0.0	0.0	0.0
−5.673	$-\frac{3}{2}$	1.0	0.0	0.0	···	−9.782	$-\frac{3}{2}$	1.0	0.0	0.0	···
−5.673	$\frac{5}{2}$	1.0	···	0.0	···	−9.782	$\frac{5}{2}$	1.0	···	0.0	···
−5.673	$-\frac{7}{2}$	1.0	···	···	···	−9.782	$-\frac{7}{2}$	1.0	···	···	···
−2.934	$\frac{1}{2}$	0.0	0.0	1.0	0.0						
−2.934	$-\frac{3}{2}$	0.0	0.0	1.0	···	−7.839	$\frac{1}{2}$	0.0	1.0	0.0	0.0
−2.934	$\frac{5}{2}$	0.0	···	1.0	···	−7.839	$-\frac{3}{2}$	0.0	1.0	0.0	···
−2.878	$\frac{1}{2}$	0.0	1.0	0.0	0.0	−6.639	$\frac{1}{2}$	0.0	0.0	1.0	0.0
−2.878	$-\frac{3}{2}$	0.0	1.0	0.0	···	−6.639	$-\frac{3}{2}$	0.0	0.0	1.0	···
−1.060	$\frac{1}{2}$	0.0	0.0	0.0	1.0	−6.639	$\frac{5}{2}$	0.0	···	1.0	···
						−6.479	$\frac{1}{2}$	0.0	0.0	0.0	1.0

TABLE III (*continued*)

(e) Ti^{50}, axial, prolate.

Protons						Neutrons					
ϵ_k	k	$f_{7/2,k}$	$P_{3/2,k}$	$f_{5/2,k}$	$P_{1/2,k}$	ϵ_k	k	$f_{7/2,k}$	$P_{3/2,k}$	$f_{5/2,k}$	$P_{1/2,k}$
−9.178	$\frac{1}{2}$	0.777	−0.544	−0.206	0.242	−14.122	$\frac{1}{2}$	0.780	−0.510	−0.260	0.255
						−11.865	$-\frac{3}{2}$	0.963	−0.205	0.174	···
−7.647	$-\frac{3}{2}$	0.941	−0.248	0.230	···	−10.632	$\frac{5}{2}$	−0.992	···	0.123	···
−5.827	$\frac{5}{2}$	−0.988	···	0.156	···	−10.137	$\frac{1}{2}$	−0.612	−0.501	−0.457	0.406
−5.646	$\frac{1}{2}$	−0.559	−0.378	−0.592	0.442						
−4.065	$\frac{7}{2}$	1.0	···	···	···	−9.835	$-\frac{7}{2}$	1.0	···	···	···
−3.963	$\frac{1}{2}$	0.283	0.670	−0.686	0.012	−8.587	$\frac{1}{2}$	0.126	0.653	−0.724	0.182
−3.227	$-\frac{3}{2}$	−0.336	−0.614	0.715	···	−8.378	$-\frac{3}{2}$	0.243	0.939	−0.243	···
−2.162	$-\frac{3}{2}$	0.036	0.750	0.661	···	−7.145	$-\frac{3}{2}$	0.114	−0.276	−0.954	···
−0.852	$\frac{1}{2}$	0.065	0.336	0.370	0.864	−6.747	$\frac{1}{2}$	0.032	0.250	0.446	0.859
−0.341	$\frac{5}{2}$	0.156	···	0.988	···	−5.749	$\frac{5}{2}$	0.123	···	0.992	···

(f) Cr^{54}, axial, prolate.

Protons						Neutrons					
ϵ_k	k	$f_{7/2,k}$	$P_{3/2,k}$	$f_{5/2,k}$	$P_{1/2,k}$	ϵ_k	k	$f_{7/2,k}$	$P_{3/2,k}$	$f_{5/2,k}$	$P_{1/2,k}$
−10.703	$\frac{1}{2}$	0.841	−0.477	−0.163	0.198	−15.887	$\frac{1}{2}$	0.821	−0.485	−0.202	0.222
−9.455	$-\frac{3}{2}$	0.931	−0.213	0.296	···	−14.250	$-\frac{3}{2}$	0.941	−0.219	0.257	···
						−12.959	$\frac{1}{2}$	0.446	0.257	0.762	−0.392
−7.842	$\frac{1}{2}$	0.379	0.239	0.819	−0.357	−12.133	$\frac{5}{2}$	−0.997	···	0.075	···
−7.300	$\frac{5}{2}$	−0.995	···	0.099	···	−11.135	$-\frac{7}{2}$	1.0	···	···	···
−6.348	$-\frac{7}{2}$	1.0	···	···	···						
−5.086	$-\frac{3}{2}$	0.355	0.344	−0.869	···	−10.151	$\frac{1}{2}$	−0.356	−0.798	0.485	0.014
−5.033	$\frac{1}{2}$	−0.386	−0.796	0.455	0.101	−9.988	$-\frac{3}{2}$	0.337	0.552	−0.763	···
−3.814	$-\frac{3}{2}$	−0.083	−0.915	−0.396	···	−8.960	$-\frac{3}{2}$	−0.026	−0.804	−0.594	···
−3.435	$\frac{5}{2}$	0.099	···	0.995	···	−8.069	$\frac{5}{2}$	0.075	···	0.997	···
−2.473	$\frac{1}{2}$	0.009	0.286	0.308	0.907	−8.042	$\frac{1}{2}$	−0.003	0.247	0.378	0.892

(g) Fe^{56}, axial, oblate.

Protons						Neutrons					
ϵ_k	k	$f_{7/2,k}$	$P_{3/2,k}$	$f_{5/2,k}$	$P_{1/2,k}$	ϵ_k	k	$f_{7/2,k}$	$P_{3/2,k}$	$f_{5/2,k}$	$P_{1/2,k}$
−11.542	$-\frac{7}{2}$	1.0	···	···	···	−17.083	$-\frac{7}{2}$	1.0	···	···	···
−9.558	$\frac{5}{2}$	0.783	···	0.622	···	−15.114	$\frac{5}{2}$	0.796	···	0.605	···
−9.347	$-\frac{3}{2}$	0.738	0.661	0.139	···	−14.829	$-\frac{3}{2}$	0.762	0.633	0.137	···
						−14.410	$\frac{1}{2}$	0.753	0.466	0.257	0.387
−8.857	$\frac{1}{2}$	0.736	0.485	0.259	0.396	−12.309	$\frac{5}{2}$	0.605	···	−0.796	···
−6.645	$\frac{5}{2}$	0.622	···	−0.783	···						
−6.166	$-\frac{3}{2}$	0.618	−0.577	−0.534	···	−11.963	$-\frac{3}{2}$	0.612	−0.636	−0.470	···
−5.643	$\frac{1}{2}$	0.605	−0.159	−0.482	−0.614	−11.587	$\frac{1}{2}$	0.614	−0.244	−0.415	−0.626
−3.728	$\frac{1}{2}$	−0.292	0.787	−0.540	−0.068	−9.609	$\frac{1}{2}$	−0.221	0.798	−0.533	−0.175
−3.415	$-\frac{3}{2}$	0.272	−0.480	0.834	···	−9.198	$-\frac{3}{2}$	0.210	−0.442	0.872	···
−1.674	$\frac{1}{2}$	0.089	−0.348	−0.640	0.679	−7.881	$\frac{1}{2}$	0.083	−0.296	−0.691	0.654

(h) Ni^{58}, axial, oblate.

Protons						Neutrons					
ϵ_k	k	$f_{7/2,k}$	$P_{3/2,k}$	$f_{5/2,k}$	$P_{1/2,k}$	ϵ_k	k	$f_{7/2,k}$	$P_{3/2,k}$	$f_{5/2,k}$	$P_{1/2,k}$
−12.412	$-\frac{7}{2}$	1.0	···	···	···	−18.734	$-\frac{7}{2}$	1.0	···	···	···
−10.628	$-\frac{3}{2}$	0.649	0.740	0.175	···	−17.131	$-\frac{3}{2}$	0.656	0.730	0.192	···
−10.231	$\frac{5}{2}$	0.760	···	0.650	···	−16.555	$\frac{5}{2}$	0.733	···	0.680	···
−9.772	$\frac{1}{2}$	0.647	0.521	0.279	0.482	−16.401	$\frac{1}{2}$	0.639	0.503	0.299	0.499
						−13.193	$\frac{5}{2}$	0.680	···	−0.733	···
−6.945	$\frac{5}{2}$	0.650	···	−0.760	···						
−6.577	$-\frac{3}{2}$	0.716	−0.518	−0.468	···	−12.934	$-\frac{3}{2}$	0.727	−0.542	−0.422	···
−6.071	$\frac{1}{2}$	0.690	−0.093	−0.417	−0.584	−12.702	$\frac{1}{2}$	0.717	−0.120	−0.388	−0.566
−3.877	$\frac{1}{2}$	−0.315	0.787	−0.513	−0.132	−10.405	$\frac{1}{2}$	−0.271	0.815	−0.476	−0.189
−3.449	$-\frac{3}{2}$	0.256	−0.429	0.867	···	−9.757	$-\frac{3}{2}$	0.204	−0.416	0.886	···
−1.555	$\frac{1}{2}$	0.078	−0.316	−0.696	0.640	−8.302	$\frac{1}{2}$	0.057	−0.262	−0.730	0.628

(i) Ni^{56}, axial, prolate.

Protons						Neutrons					
ϵ_k	k	$f_{7/2,k}$	$P_{3/2,k}$	$f_{5/2,k}$	$P_{1/2,k}$	ϵ_k	k	$f_{7/2,k}$	$P_{3/2,k}$	$f_{5/2,k}$	$P_{1/2,k}$
−11.774	$\frac{1}{2}$	0.794	−0.571	−0.086	0.190	−18.946	$\frac{1}{2}$	0.806	−0.556	−0.082	0.188

TABLE III (*continued*)

(i) Ni^{56}, axial, prolate.

Protons						Neutrons					
ϵ_k	k	$f_{7/2,k}$	$P_{3/2,k}$	$f_{5/2,k}$	$P_{1/2,k}$	ϵ_k	k	$f_{7/2,k}$	$P_{3/2,k}$	$f_{5/2,k}$	$P_{1/2,k}$
−10.504	$-\frac{3}{2}$	0.909	−0.313	0.276	···	−17.748	$-\frac{3}{2}$	0.912	−0.303	0.276	···
−8.283	$\frac{1}{2}$	0.385	0.265	0.742	−0.481	−15.535	$\frac{1}{2}$	−0.369	−0.260	−0.748	0.487
−7.561	$\frac{5}{2}$	−0.980	···	0.199	···	−14.828	$\frac{5}{2}$	−0.980	···	0.199	···
−5.095	$\frac{1}{2}$	−0.462	−0.698	0.541	0.080	−12.298	$-\frac{3}{2}$	−0.370	−0.317	0.873	···
−5.060	$-\frac{3}{2}$	−0.381	−0.349	0.856	···	−12.238	$-\frac{7}{2}$	1.0	···	···	···
−4.974	$-\frac{7}{2}$	1.0	···	···	···	−12.232	$\frac{1}{2}$	0.455	0.702	−0.537	−0.106
−3.013	$-\frac{3}{2}$	0.172	0.883	0.437	···	−10.059	$-\frac{3}{2}$	0.177	0.899	0.401	···
−1.572	$\frac{1}{2}$	0.083	0.342	0.387	0.852	−8.814	$\frac{1}{2}$	0.090	0.361	0.381	0.847
−1.159	$\frac{5}{2}$	0.199	···	0.980	···	−8.422	$\frac{5}{2}$	0.199	···	0.980	···

(j) Ni^{56}, axial, oblate.

Protons						Neutrons					
ϵ_k	k	$f_{7/2,k}$	$P_{3/2,k}$	$f_{5/2,k}$	$P_{1/2,k}$	ϵ_k	k	$f_{7/2,k}$	$P_{3/2,k}$	$f_{5/2,k}$	$P_{1/2,k}$
−11.230	$-\frac{7}{2}$	1.0	···	···	···	−18.500	$-\frac{7}{2}$	1.0	···	···	···
−9.851	$-\frac{3}{2}$	0.589	0.781	0.210	···	−16.956	$-\frac{3}{2}$	0.606	0.767	0.211	···
−8.878	$\frac{1}{2}$	0.591	0.527	0.299	0.533	−16.076	$\frac{1}{2}$	0.596	0.511	0.302	0.541
−8.651	$\frac{5}{2}$	0.710	···	0.704	···	−15.920	$\frac{5}{2}$	0.710	···	0.704	···
−5.369	$\frac{5}{2}$	0.704	···	−0.710	···	−12.638	$\frac{5}{2}$	0.704	···	−0.710	···
−4.930	$-\frac{3}{2}$	0.800	−0.526	−0.289	···	−12.118	$-\frac{3}{2}$	0.786	−0.536	−0.309	···
−4.839	$\frac{1}{2}$	−0.765	0.130	0.357	0.519	−12.110	$\frac{1}{2}$	−0.760	0.115	0.362	0.527
−2.758	$\frac{1}{2}$	0.255	−0.819	0.425	0.288	−9.836	$\frac{1}{2}$	0.258	−0.827	0.427	0.259
−1.712	$-\frac{3}{2}$	0.115	−0.338	0.934	···	−8.941	$-\frac{3}{2}$	0.124	−0.353	0.928	···
−0.301	$\frac{1}{2}$	0.015	−0.187	−0.776	0.602	−7.547	$\frac{1}{2}$	0.019	−0.204	−0.772	0.602

(k) Cr^{48}, triaxial.

ϵ_λ	HF orbitals for protons										
−7.85317	0.794	−0.499	−0.187	0.212	0.151	−0.058	0.105	−0.058	0.010	−0.005	
−6.01081	0.070	0.186	0.373	−0.226	0.825	−0.209	0.205	0.054	−0.016	−0.023	
−3.77188	0.353	0.243	0.158	−0.169	−0.230	0.056	−0.058	0.834	−0.085	0.014	
−3.14733	−0.440	−0.355	−0.441	0.292	0.333	−0.064	0.047	0.530	−0.026	−0.034	
−2.62610	0.008	0.002	0.016	−0.016	−0.063	−0.070	0.018	−0.005	−0.000	−0.995	
−1.72604	−0.199	−0.577	0.513	−0.160	−0.299	−0.428	0.235	0.083	−0.014	0.061	
−1.09286	0.080	0.370	−0.360	0.064	−0.143	−0.827	0.113	−0.037	0.007	0.064	
0.36275	0.018	−0.224	−0.114	−0.444	0.128	−0.218	−0.820	−0.023	−0.053	−0.002	
0.94731	−0.011	−0.100	−0.444	−0.736	−0.048	0.161	0.448	−0.039	−0.143	0.004	
2.00692	−0.008	0.018	0.051	0.146	0.003	−0.012	−0.022	−0.082	−0.984	−0.000	
ϵ_λ	HF orbitals for neutrons										
−15.05805	0.804	−0.482	−0.184	0.211	0.159	−0.058	0.107	−0.057	0.010	−0.005	
−13.26486	0.056	0.184	0.377	−0.230	0.826	−0.199	0.204	0.055	−0.016	−0.023	
−11.02573	0.329	0.221	0.156	−0.169	−0.222	0.049	−0.055	0.853	−0.086	0.013	
−10.38331	−0.435	−0.335	−0.473	0.313	0.349	−0.055	0.045	0.499	−0.022	−0.034	
−9.88556	0.007	0.002	0.015	−0.015	−0.058	−0.060	0.017	−0.004	−0.000	−0.996	
−8.85349	−0.219	−0.615	0.508	−0.131	−0.276	−0.381	0.258	0.090	−0.012	0.050	
−8.13119	0.072	0.351	−0.331	0.040	−0.159	−0.840	0.159	−0.034	0.005	0.059	
−6.87595	0.011	−0.243	−0.119	−0.455	0.119	−0.249	−0.800	−0.021	−0.055	−0.001	
−6.31018	−0.014	−0.108	−0.438	−0.727	−0.046	0.187	0.457	−0.038	−0.142	0.003	
−5.25186	−0.008	0.020	0.051	0.146	0.002	−0.013	−0.022	−0.082	−0.984	−0.000	

(l) Fe^{56}, triaxial.

ϵ_λ	HF orbitals for protons										
−11.74419	−0.829	0.509	0.096	−0.192	0.078	−0.022	0.023	0.025	−0.008	−0.001	
−10.58906	−0.070	0.051	−0.026	−0.011	−0.918	0.242	−0.299	0.007	−0.002	0.002	
−8.36229	−0.311	−0.257	−0.726	0.365	0.019	−0.006	0.026	0.415	−0.055	−0.002	
−7.97018	0.165	0.098	0.333	−0.168	−0.007	0.000	−0.003	0.901	−0.112	0.002	
−6.74003	0.002	0.003	0.001	0.001	0.022	0.020	−0.060	0.001	−0.000	−0.998	
−5.43373	0.378	0.662	−0.428	−0.088	−0.161	−0.192	0.404	0.002	0.014	−0.029	

TABLE III (*continued*)

(l) Fe^{56}, triaxial

ϵ_λ	HF orbitals for protons											
−5.39342	0.200	0.358	−0.239	−0.023	0.333	0.278	−0.763	0.009	0.007	0.060		
−4.16047	0.015	0.022	−0.019	−0.028	0.110	0.909	0.400	−0.003	−0.010	−0.004		
−3.48354	0.014	0.040	0.025	0.082	−0.001	−0.009	−0.003	−0.124	−0.988	0.000		
−2.65216	0.021	0.307	0.331	0.887	−0.008	0.018	0.024	0.017	0.093	0.001		
ϵ_λ	HF orbitals for neutrons											
−18.13106	0.811	−0.526	−0.123	0.219	−0.031	0.010	−0.008	−0.028	0.006	0.000		
−16.62618	−0.041	0.019	−0.055	0.013	−0.919	0.251	−0.295	0.003	−0.002	−0.005		
−14.52492	−0.397	−0.257	−0.765	0.432	0.046	−0.019	0.041	0.029	−0.008	−0.001		
−13.53878	0.042	0.002	0.010	−0.014	−0.001	−0.001	0.006	0.992	−0.115	0.000		
−11.96279	0.004	0.005	−0.003	0.001	0.019	−0.017	−0.056	0.001	−0.000	−0.998		
−11.19365	0.421	0.743	−0.502	−0.053	0.063	0.019	−0.102	−0.013	0.013	0.013		
−10.97950	0.058	0.087	−0.047	−0.034	−0.377	−0.442	0.804	−0.009	0.002	−0.044		
−9.78624	0.014	0.024	−0.012	−0.012	0.075	0.861	0.501	−0.003	−0.004	−0.042		
−8.65870	0.021	0.194	0.228	0.528	−0.006	−0.004	0.009	−0.087	−0.789	0.000		
−8.64767	0.012	0.241	0.302	0.694	−0.009	0.002	0.016	0.075	0.603	−0.000		

(m) Ni^{58}, triaxial.

ϵ_λ	HF orbitals for protons									
−12.85313	−0.798	0.522	0.045	−0.119	−0.243	0.106	−0.033	−0.039	0.029	0.008
−11.76985	−0.133	0.227	0.107	−0.176	0.858	−0.326	0.213	0.005	0.004	−0.033
−9.93553	−0.252	−0.359	0.014	0.242	0.065	−0.046	0.099	−0.832	0.203	−0.008
−9.03210	0.333	0.228	0.680	−0.477	−0.156	0.039	−0.072	−0.337	0.051	0.011
−7.47891	−0.256	−0.417	0.467	0.018	−0.214	−0.211	0.580	0.317	−0.075	−0.095
−6.19258	−0.099	−0.149	0.156	0.022	0.134	0.204	−0.049	0.083	−0.020	0.935
−5.49805	0.268	0.382	−0.352	−0.025	−0.255	−0.219	0.655	−0.184	0.034	0.285
−4.11174	−0.087	−0.129	−0.103	−0.201	−0.217	−0.829	−0.395	−0.005	−0.028	0.184
−2.71705	0.121	0.321	0.341	0.683	−0.026	−0.220	−0.111	0.140	0.466	0.035
−1.78351	0.037	0.181	0.177	0.400	0.000	−0.094	−0.053	−0.179	−0.855	0.009
ϵ_λ	HF orbitals for neutrons									
−19.36665	−0.802	0.545	0.062	−0.155	−0.157	0.066	−0.025	−0.031	0.023	0.007
−18.24885	−0.081	0.146	0.064	−0.124	0.890	−0.322	0.237	0.016	−0.005	−0.028
−16.03286	0.304	0.358	0.169	−0.330	−0.059	0.040	−0.117	0.768	−0.183	0.005
−15.62769	0.275	0.148	0.678	−0.423	−0.098	−0.004	−0.006	−0.497	0.085	−0.005
−13.59221	0.284	0.444	−0.447	−0.046	0.214	0.210	−0.566	−0.307	0.063	0.108
−12.80609	0.070	0.114	−0.124	−0.015	−0.086	−0.156	−0.020	−0.054	0.009	−0.965
−11.96537	0.276	0.410	−0.358	−0.026	−0.284	−0.276	0.647	−0.137	0.025	0.179
−10.62497	−0.079	−0.126	−0.076	−0.160	−0.191	−0.841	−0.421	−0.009	−0.047	0.153
−9.35223	−0.112	−0.332	−0.359	−0.715	0.009	0.191	0.113	−0.120	−0.416	−0.022
−8.47939	0.029	0.161	0.162	0.366	0.006	−0.045	−0.032	−0.178	−0.882	0.004

two-body term in Eq. (1), it would make h less attractive, hence give less binding in the total HF energy.

Levinson[12] gives a rough extrapolation of the gap between occupied and unoccupied levels as $G \cong 80/A$ MeV. For the range of nuclei studied here, $A=40$ to 60, G ranges from 2 MeV down to 1.3 MeV. The gaps given in the last two columns in Table II show in most cases approximate agreement with this rule for the lowest-energy solution.

In Table III and Figs. 1 and 2 are given the HF single-particle orbitals for some representative cases. These wave functions can be tested by stripping and pickup reactions. The total pickup strengths for neutrons and protons are given in Table IV. These were obtained by taking the sum $\sum_{\nu m}|C_{jm}{}^{\nu}|^2$ [see Eq. (2)] over all occupied orbitals ν. The tables therefore show the fractional occupation of each spherical single-particle orbital. These numbers are in over-all agreement with the experiments except in the following few cases. In nuclei where we have eight neutrons outside of Ca^{40} (Ti^{50}, Cr^{52}, Fe^{54}, Ni^{56}), the largest component in the neutron wave function is not $(f_{7/2})^8$ as one might expect on a shell-model basis. The reason is that for eight neutrons the occupied orbitals[13] are $k=\pm\frac{1}{2}$, $\pm\frac{3}{2}$,

[12] C. A. Levinson, in *Proceedings of the Twelfth International Summer Meeting in Physics, Herzeg Novi, Yugoslavia*, edited by M. V. Mihailovic, M. Rosina, and J. Strand (The Federal Nuclear Energy Commission of Yugoslavia, Beograd, 1967), p. 43.

[13] k denotes the projection of the single-particle angular momentum on the symmetry axis.

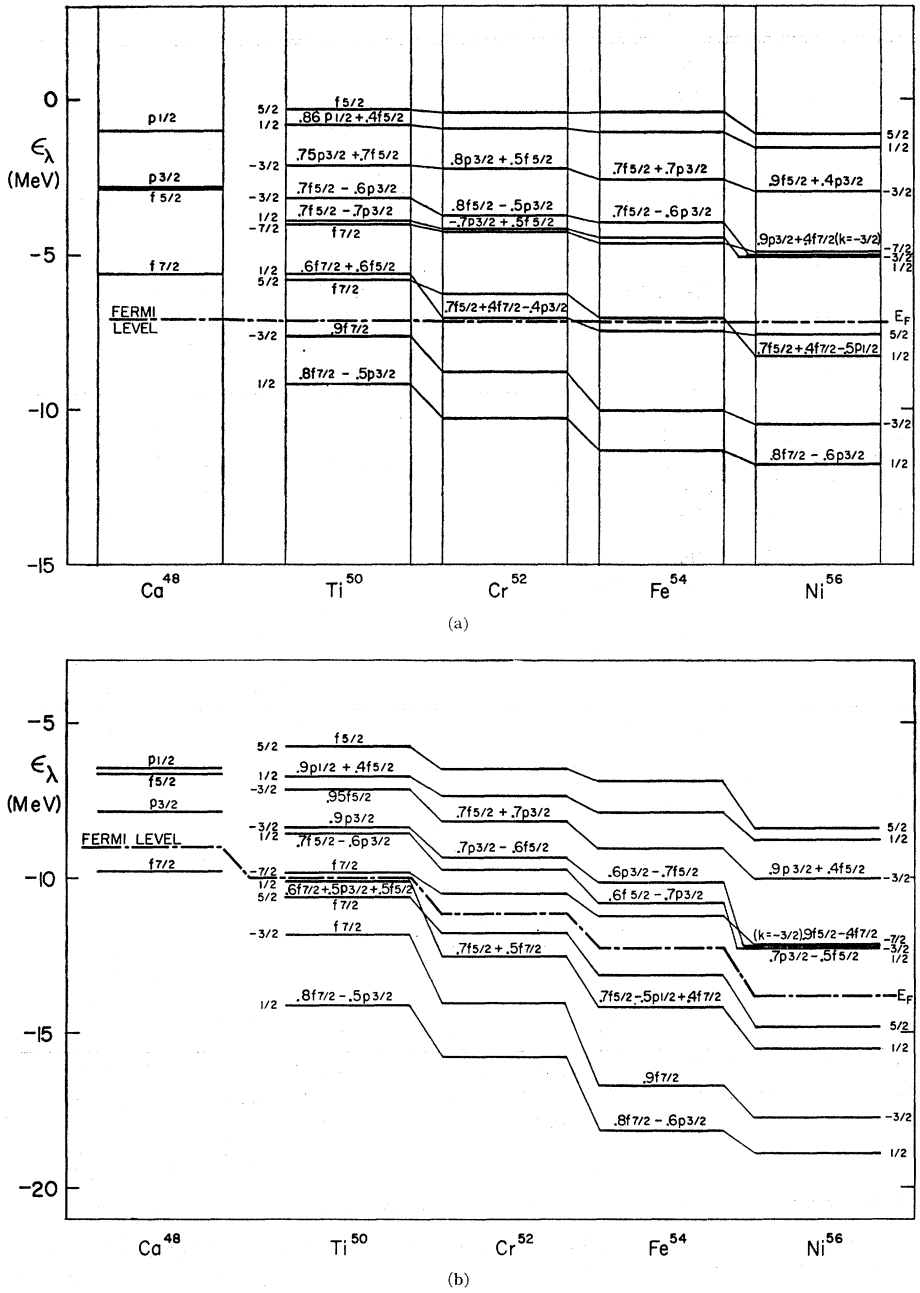

FIG. 2. (a) Proton and (b) neutron single-particle levels in $N=28$ nuclei. Ca^{48} is spherical, so all levels have pure j and the various k values belonging to the same j are degenerate. In the other isotopes, the labeling is as in Fig. 1.

$\pm\frac{1}{2}'$, and $\pm\frac{5}{2}$, with $k=\pm\frac{7}{2}$ being the lowest unoccupied orbital. Therefore, in these cases one cannot get an $(f_{7/2})^8$ component in the wave function. However, when there are more than eight neutrons this would be possible because $k=\pm\frac{7}{2}$ would be occupied.

(*a*) *Calcium isotopes.* $Ca^{42,44,46}$ have essentially no gap between the occupied and unoccupied neutron orbitals. The proton gap is just the shell gap between the $2s$-$1d$ and $2p$-$1f$ shells. They are all deformed, but only slightly; the admixture of orbitals of different j are very small. The occupied neutron orbitals are quite pure $f_{7/2}$, the purity increasing with increasing number of neutrons. Neutron and proton orbitals are very similar. Ca^{48} is spherical, the $f_{7/2}$ neutron shell being fully occupied. The neutron gap is just the spacing between the $f_{7/2}$ and $p_{3/2}$ single-particle levels.

(*b*) *Titanium isotopes.* Addition of two protons and two neutrons outside an inert Ca^{40} core gives a large intrinsic quadrupole moment (hence large deformation). This is in contrast to the situation in Ca^{44} where the valence particles are four neutrons and the intrinsic quadrupole moment is smaller by a factor of 2. The occupied orbitals in Ca isotopes are pure $f_{7/2}$ type, whereas in Ti isotopes there is a considerable admixture

of other spherical orbitals, $(p_{3/2},f_{5/2},p_{1/2})$. This can be seen from the total pickup strengths (Table IV). In Ti^{48} and in Ca^{46} the occupied neutron orbitals are $k=\frac{1}{2}$, $-\frac{3}{2}$, and $\frac{5}{2}$. However, the eight neutrons in Ti^{50} do not fill the $f_{7/2}$ shell as they did in Ca^{48}, but a second $k=\frac{1}{2}$ orbital comes below the $k=-\frac{7}{2}$. This difference in the structure of orbitals between the Ca and the Ti isotopes must be due to the neutron-proton force.

(*c*) *Chromium isotopes.* With four protons outside Ca^{40}, we again get a deformed $k=\frac{1}{2}$ orbit. For prolate solutions, the proton occupation is $k=\frac{1}{2}$, $-\frac{3}{2}$, and $\frac{1}{2}'$. The oblate solutions lie higher in energy than the prolate ones and are more deformed than the oblate solutions in the Ti isotopes. In the prolate solution in Cr^{52}, the eight neutrons again do not fully occupy the $f_{7/2}$ shell, but the $k=(\frac{1}{2})'$ state comes below the $k=-\frac{7}{2}$ one. This is an indication that the SU_3 scheme is good. Both the $k=\frac{1}{2}$ and $k=(\frac{1}{2})'$ levels are made up of mostly the ϕ_0 and $\phi_{\pm1}$ SU_3 orbitals [see Eq. (8)]. These are the lowest levels in the SU_3 scheme. The $k=-\frac{3}{2}$ orbit can also be made up of the $\phi_{\pm1}$ state, but the $k=-\frac{7}{2}$ orbit involves $\phi_{\pm3}$, which is the highest SU_3 state. Hence the $k=\frac{1}{2}$, $-\frac{3}{2}$, $(\frac{1}{2})'$ levels are lower than the $k=-\frac{7}{2}$ one.

(*d*) *Iron isotopes.* The structure and occupation of the orbits are quite similar to what is observed in the Cr isotopes. The *f*-*p* mixing is less in the prolate solutions, but about the same in the oblate ones, as that seen in the prolate Cr isotopes.

(*e*) *Nickel isotopes.* With eight protons and eight neutrons outside Ca^{40}, a large gap (2.5 MeV) between occupied and unoccupied states is seen. In some sense, therefore, there appears to be a shell closure at Ni^{56}, but it is not a closed $f_{7/2}$ shell, and it is not spherical. In Ni^{56} the prolate solution is slightly lower, in Ni^{58} the oblate, but in Ni^{58} a still lower triaxial solution was found. The structure and occupation of the single-particle levels is similar to previous cases.

(*f*) *Spherical nuclei.* HF calculation were also carried out for the nuclei Ca^{40}, Ca^{48}, and Ni^{56} under the assumption that they are spherical.[14] In this case, no inert core was assumed, but all the A particles of the nucleus are included in the sums on occupied states in Eqs. (1) and (4). Then, the single-particle energies, e_j in Eqs. (1) and (4), are replaced by the single-particle kinetic energy $\langle j_1m_1|(p^2/2M)|j_2m_2\rangle$, and the sum in Eq. (2) is over the radial quantum number n. The basis consisted of the 1*s*, 1*p*, 2*s*-1*d*, and 2*p*-1*f* harmonic-oscillator functions. These results are shown in Table V. It is clear that the binding energies are too low. The Ca^{40} binding energy is about 5 MeV per particle against the experimental value of 8.5 MeV, and the binding energies of Ca^{48} and Ni^{56} relative to Ca^{40} are much smaller than in the pure *p*-*f*-shell calculation. This seems surprising since one would expect to get more binding when using a larger basis. Even going to a still larger basis, in-

[14] A. K. Kerman, J. P. Svenne, and F. M. H. Villars, Phys. Rev. **147**, 710 (1966).

TABLE IV. Neutron (a) and proton (b) pickup strengths. The various solutions for each nucleus are listed in the same order as in Table II. Under "type," *P* denotes prolate axial, *O* oblate axial, and *T* triaxial solutions.

	Nucleus	Type	$f_{7/2}$	$p_{3/2}$	$f_{5/2}$	$p_{1/2}$
(a)	Ca^{42}	*O*	1.980	0.012	0.006	0.002
		P	2.000	0	0	0
	Ca^{44}	*P*	3.948	0.034	0.018	0.002
	Ca^{46}	*P*	5.960	0.024	0.018	0.000
	Ca^{48}	sph.	8.000	0	0	0
	Ti^{44}	*P*	1.404	0.331	0.174	0.089
		O	2.000	0	0	0
	Ti^{46}	*P*	3.247	0.422	0.229	0.102
		O	3.824	0	0.176	0
	Ti^{48}	*P*	5.278	0.383	0.253	0.087
		O	5.527	0.251	0.224	0.000
	Ti^{50}	*P*	5.789	1.106	0.644	0.460
		T	7.360	0.256	0.344	0.040
		O	7.154	0.463	0.332	0.053
	Cr^{48}	*T*	2.692	0.660	0.454	0.192
		P	3.094	0.539	0.256	0.110
		O	3.775	0	0.224	0
	Cr^{50}	*P*	3.506	0.908	1.091	0.494
		O	5.546	0.190	0.263	0
	Cr^{52}	*P*	5.436	0.838	1.239	0.485
	Cr^{54}	*P*	7.505	0.698	1.386	0.406
		O	7.358	0.592	2.014	0.041
	Fe^{52}	*P*	3.282	1.041	1.108	0.567
		01	4.345	0.842	0.814	0
		02	3.484	1.711	0.240	0.566
	Fe^{54}	*P*	5.194	0.998	1.251	0.559
		O	4.617	1.724	1.077	0.583
	Fe^{56}	*T*	7.586	0.774	1.292	0.340
		O	6.295	1.236	2.169	0.300
		P	7.402	0.370	2.154	0.075
	Ni^{56}	*P*	5.156	0.937	1.364	0.545
		O	4.453	1.699	1.263	0.585
	Ni^{58}	*T*	5.386	1.742	2.204	0.668
		O	5.677	1.572	2.252	0.498
		P	5.528	1.881	1.929	0.665
	Ni^{62}	*P*	7.876	2.172	3.276	0.682
		O	7.465	2.212	3.145	1.177
(b)	Ti^{44}	*P*	1.379	0.361	0.174	0.088
		O	2.000	0	0	0
	Ti^{46}	*P*	1.322	0.425	0.152	0.098
		O	2.000	0	0	0
	Ti^{48}	*P*	1.408	0.343	0.181	0.067
		O	2.000	0	0	0
	Ti^{50}	*P*	1.207	0.592	0.085	0.117
		T	1.835	0.002	0.163	0.000
		O	2.000	0	0	0
	Cr^{48}	*T*	2.691	0.661	0.455	0.192
		P	3.054	0.582	0.256	0.109
		O	3.775	0	0.224	0
	Cr^{50}	*P*	2.871	0.768	0.236	0.123
		O	3.538	0	0.463	0
	Cr^{52}	*P*	2.955	0.743	0.210	0.091
	Cr^{54}	*P*	3.148	0.546	0.228	0.078
		O	3.542	0	0.457	0
	Fe^{52}	*P*	3.268	1.094	1.087	0.552
		01	4.275	0.911	0.811	0
		02	3.415	1.806	0.236	0.545
	Fe^{54}	*P*	3.219	1.038	1.190	0.549
		O	3.369	1.797	0.264	0.568
	Fe^{56}	*T*	3.622	0.774	1.260	0.340
		O	4.315	0.874	0.812	0
		P	5.331	0.185	0.411	0.074
	Ni^{56}	*P*	5.131	0.988	1.347	0.535
		O	4.401	1.775	1.258	0.568
	Ni^{58}	*T*	4.922	1.260	1.160	0.664
		O	4.835	1.638	1.062	0.463
		P	5.209	1.175	0.943	0.671
	Ni^{62}	*P*	5.376	1.204	0.758	0.666
		O	5.230	1.849	0.594	0.376

TABLE V. The spherical HF solutions in Ca^{40}, Ca^{48}, and Ni^{56} with the Yale-Shakin potential. In the case of Ca^{40}, results of a calculation including the Coulomb force are also shown. All energies are in MeV, the rms radius in fermi. The column labeled Ni^{56*} is the solution, described in the text, with five protons and five neutrons in the $f_{7/2}$ level, and one each in the $2p_{3/2}$, $f_{5/2}$, and $2p_{1/2}$ states, respectively.

	Ca^{40}						
	No Coulomb force	With Coulomb force		Ca^{48}		Ni^{56}	Ni^{56*}
E_0	−201.43	−124.98		−221.01		−277.57	−270.02
$\lvert E_0-E(Ca^{40})\rvert$	0	0		19.58		76.14	68.59
rms radius	3.527	3.54		3.55		3.83	3.84
Single-particle energies		Neutron	Proton	Neutron	Proton		
$1s_{1/2}$	−56.25	−55.75	−47.25	−58.05	−60.26	−62.33	−63.69
$1p_{3/2}$	−36.12	−35.87	−27.80	−38.15	−41.34	−43.49	−44.09
$1p_{1/2}$	−33.20	−32.99	−24.96	−37.54	−40.51	−44.93	−42.69
$1d_{5/2}$	−16.81	−16.80	−9.56	−18.73	−22.28	−24.20	−24.53
$2s_{1/2}$	−14.60	−14.62	−7.54	−17.04	−20.21	−22.52	−22.71
$1d_{3/2}$	−12.75	−12.78	−5.56	−17.45	−21.25	−25.93	−22.91
$1f_{7/2}$	−1.69	−1.75	4.93	−3.22	−6.32	−7.83	−8.43
$2p_{3/2}$	−1.15	−1.12	5.32	−2.67	−5.04	−6.52	−7.66
$1f_{5/2}$	2.85			−1.09	−4.62	−8.52	−6.07
$2p_{1/2}$	0.35	0.39	6.83	−1.78	−4.09	−6.20	−6.21

cluding also the $3s$-$2d$ and $3p$-$2f$ shells, did not give significant improvement. However, it is consistent with the finding of Shakin *et al.*[6] They observe that it is necessary to include the second-order terms of the strong pseudopotentials which are needed in order to use the separation method in the P states. These second-order terms are not included in our calculation. They are probably relatively unimportant for the matrix elements within the $2p$-$1f$ shell, but important for the deeper shells, particularly the $1p$ shell. The reason for the discrepancy in binding of Ca^{48} and Ni^{56} between these and the p-f-shell calculations can also be seen from the single-particle energies of the $2p$-$1f$ shell obtained for Ca^{40}. They are about 4 to 6 MeV higher than the experimental ones (Table I), used in the p-f-shell work. Hence, when these are filled, the HF energy is too small. In Ni^{56} an additional reason for underbinding is that it is in fact not spherical but has a deformed solution at a lower energy [see (*e*), above].

In the Ni^{56} solution, an inversion of the spin-orbit partners is seen. In particular, the $f_{5/2}$ state is lower than the occupied $f_{7/2}$ one. This is a general feature of spherical HF solutions where one of the spin-orbit partners is completely occupied.[15] In those cases, the other, unoccupied level lies lower in energy than the occupied one. We have also performed a spherical HF calculation on Ni^{56} where, instead of the $f_{7/2}$ level being completely occupied and the other levels of the p-f-shell empty, we distribute the eight neutrons and eight protons over the p-f shell roughly in the proportion seen in the deformed solution [Table III(i)]; i.e., five in the $f_{7/2}$ level and one each in $p_{3/2}$, $f_{5/2}$, and $p_{1/2}$ levels. This should not be a spherical solution, but we can constrain it to be spherical. Then we obtain the results shown in the column labeled Ni^{56*} in Table V. The levels are now in more normal order. In particular, the level ordering in the p-f shell is $f_{7/2}$, $p_{3/2}$, $p_{1/2}$, $f_{5/2}$. This "solution" is, however, 7 MeV higher than the one in which the $f_{7/2}$ shell is completely filled. This decreased binding is at least in part due to the spherical constraint.

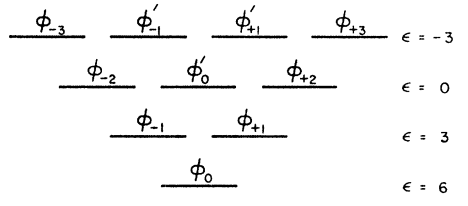

FIG. 3. Single-particle states in a quadrupole potential, $\epsilon=2\langle Q_{20}\rangle$ in units of b^2.

[15] C. W. Wong, Nucl. Phys. A108, 481 (1968).

III. INFINITE-RANGE FORCE

The results with the infinite-range force [Eq. (5)] show the gross structure of these nuclei. Bar-Touv and Levinson[9] perform these calculations with the single-particle energies e_{lj} all zero (no spin-orbit force). Since, in the p-f shell, the spin-orbit force is expected[3] to play an important role, we have also done the infinite-range calculation with nonzero spin-orbit force, the e_{lj} being taken as in Table I. In order that there be a proper balance between the one- and two-body parts of the HF Hamiltonian [Eq. (1)], the strength V_0 of the infinite-range force was taken as 2.57 MeV so that the Ti^{44} binding energy is nearly the same as with the finite-range force. We discuss the zero and finite spin-orbit results separately.

(*a*) *Zero spin-orbit force.* The calculation with the infinite-range force, and all e_{lj} equal to zero, should yield the zero-order scheme for these nuclei. There should be a constant gap[9] between occupied and unoccupied levels for $N=Z$:

$$G=-(W+2B-4M-2H)=4.55\ \text{MeV}. \quad (7)$$

All the orbitals of the same type—occupied or unoccupied—should be degenerate. This is in fact observed in the calculations. In Ti^{44}, we find the occupied

TABLE VI. Results of the HF calculation with the infinite-range force and nonzero spin-orbit interaction. The HF energy (E_{HF}), mass quadrupole moment (Q_{20}, in units of b^2), proton and neutron gaps (G_p,G_n), and structure of the occupied orbits are shown. All energies are in MeV. The values of k for the occupied orbits and their dominant coefficients are shown. In the cases of neutron excess, the states having only neutrons are indicated by (n) after their k value (except for Ca^{48}). In the neutron and proton orbitals essentially different in structure, this is indicated by the lables (n) or (p).

Nucleus	$-E_{HF}$	Q_{20}	G_p	G_n	Occupied orbitals k	Occupied orbitals Main terms
Ca^{48}	32.17	−0.16		5.09	$\frac{1}{2}, -\frac{3}{2}$	
					$\frac{5}{2}, -\frac{7}{2}$	$f_{7/2}$—spherical
	29.32	4.09		2.18	$-\frac{3}{2}, -\frac{7}{2}$	$f_{7/2}$
					$\frac{1}{2}$	$0.8f_{7/2}-0.4p_{3/2}$
					$\frac{1}{2}$	$0.5f_{7/2}+0.8p_{3/2}-0.4p_{1/2}$
	25.32	10.56		0.66	$\frac{1}{2}, -\frac{3}{2}$	$f_{7/2}$
					$\frac{1}{2}$	$-0.9p_{3/2}+0.5p_{1/2}$
					$\frac{1}{2}$	$f_{5/2}$
Ti^{44}	29.74	5.19	9.18	9.19	$\frac{1}{2}$	$0.9f_{7/2}-0.5f_{5/2}$
	22.20	3.12	1.48	1.48	$-\frac{3}{2}$	$f_{7/2}$
Ti^{50}	44.41	1.36	1.18	4.70	$-\frac{3}{2}$	$f_{7/2}$
					$\frac{1}{2}(n)$	$0.9f_{7/2}+0.5f_{5/2}$
					$-\frac{7}{2}(n)$	
					$\frac{5}{2}(n)$	$f_{7/2}$
Ti^{50}	41.07	12.25	4.87	2.00	$\frac{1}{2}$	$0.9f_{7/2}-0.3f_{5/2}$
					$-\frac{3}{2}(n)$	$0.9f_{7/2}+0.3f_{5/2}$
					$\frac{1}{2}(n)$	$0.9p_{3/2}-0.5p_{1/2}$
					$\frac{1}{2}(n)$	$0.9f_{5/2}+0.3f_{7/2}$
Cr^{48}	48.22	7.63	8.54	8.54	$-\frac{3}{2}$	$0.9f_{7/2}+0.4f_{5/2}$
					$\frac{1}{2}$	$0.8f_{7/2}+0.5f_{5/2}$
	36.65	−2.88	1.48	1.48	$-\frac{7}{2}$	
					$-\frac{3}{2}$	$f_{7/2}$
Cr^{52}	51.36	−3.57	1.06	5.19	$-\frac{7}{2}$	$f_{7/2}$
					$-\frac{3}{2}$	$0.95f_{7/2}+0.3f_{5/2}$
					$\frac{1}{2}(n)$	$0.9f_{7/2}+0.5f_{5/2}$
					$\frac{5}{2}(n)$	$0.7f_{7/2}+0.7f_{5/2}$
	49.87	13.88	6.15	3.21	$-\frac{3}{2}$	$0.9f_{7/2}+0.4f_{5/2}$
					$\frac{1}{2}$	$0.95f_{7/2}+0.3f_{5/2}$
					$\frac{1}{2}(n)$	$0.9p_{3/2}-0.5p_{1/2}$
					$\frac{1}{2}(n)$	$0.97f_{5/2}-0.25f_{7/2}$
Fe^{52}	52.57	14.79	8.43	8.38	$-\frac{3}{2}$	$0.9f_{7/2}+0.4f_{5/2}$
					$\frac{1}{2}$	$0.4f_{7/2}-0.8p_{3/2}+0.4p_{1/2}$
					$\frac{1}{2}$	$0.7f_{7/2}+0.4p_{3/2}+0.5f_{5/2}$
Fe^{54}	51.08	17.38	6.14	3.21	$-\frac{3}{2}$	$0.9f_{7/2}+0.4f_{5/2}$
					$\frac{1}{2}$	(p) $0.5f_{7/2}+0.7p_{3/2}-0.4p_{1/2}$
						(n) $0.9p_{3/2}-0.5p_{1/2}$
					$\frac{1}{2}$	(p) $0.8f_{7/2}-0.4p_{3/2}+0.3f_{5/2}$
						(n) $f_{7/2}$
					$\frac{1}{2}(n)$	$f_{5/2}$
	50.60	−19.94	3.73	4.80	$-\frac{3}{2}$	$0.5f_{7/2}+0.8p_{3/2}$
					$\frac{1}{2}$	$0.5f_{7/2}+0.5p_{3/2}+0.6p_{1/2}$
					$-\frac{7}{2}$	$f_{7/2}$
					$\frac{5}{2}(n)$	$0.7f_{7/2}+0.7f_{5/2}$
Ni^{56}	49.65	−5.28	7.82	7.82	$-\frac{7}{2}$	$f_{7/2}$
					$-\frac{3}{2}$	$0.9f_{7/2}+0.4f_{5/2}$
					$\frac{1}{2}$	$0.8f_{7/2}+0.5f_{5/2}$
					$\frac{5}{2}$	$0.6f_{7/2}+0.8f_{5/2}$
	43.86	21.77	5.97	5.97	$\frac{1}{2}$	$f_{7/2}$
					$-\frac{3}{2}$	$0.9f_{7/2}+0.4f_{5/2}$
					$\frac{1}{2}$	$0.9p_{3/2}-0.5p_{1/2}$
					$\frac{1}{2}$	$f_{5/2}$
Ni^{58}	42.74	−5.05	4.18	2.34	$-\frac{7}{2}, -\frac{3}{2}$	$f_{7/2}$
					$\frac{1}{2}$	$0.8f_{7/2}+0.5f_{5/2}$
					$\frac{5}{2}$	$0.7f_{7/2}+0.7f_{5/2}$
					$\frac{5}{2}(n)$	$0.7f_{7/2}-0.7f_{5/2}$

TABLE VII. Energy (in MeV) of the β and the γ vibrational state in Ti^{44}, for different values of the strength parameter α.

α	$\hbar\omega(\mu=0)$	$\hbar\omega(\mu=2)$
1	4.008	2.283
2	3.838	2.200
3	3.661	2.112

levels at -3.474 MeV and the unoccupied ones at $+1.075$ MeV, 4.55 MeV above the occupied ones.

As in the *s-d* shell,[2,9] axial and triaxial solutions alternate: Ti^{44}, Fe^{52}, and Ni^{56} are axial, Cr^{48} is triaxial. This is easiest explained by observing the SU_3 scheme of levels in a quadrupole well,[3] as shown in Fig. 3. The $2p$-$1f$-shell oscillator functions are shown below in a convenient representation.

$$\begin{aligned}
\phi_0&=(\sqrt{2}f_0-\sqrt{3}p_0)/\sqrt{5},\\
\phi_{\pm1}&=(2f_{\pm1}-p_{\pm1})/\sqrt{5},\\
\phi_{\pm2}&=f_{\pm2},\\
\phi_0'&=(\sqrt{3}f_0+\sqrt{2}p_0)/\sqrt{5},\\
\phi_{\pm3}&=f_{\pm3},\\
\phi_{\pm1}'&=(f_{\pm1}+2p_{\pm1})/\sqrt{5}.
\end{aligned}\tag{8}$$

Here the subscripts label the projection of the orbital angular momentum on the symmetry axis; f and p are, respectively, the spherical oscillator functions for the $1f$ and $2p$ states. If the field-producing forces tend to lead to an average quadrupole field, then these zero-order levels would fill in order of decreasing $\epsilon=2\langle Q_{20}\rangle$ to maximize the prolate deformation. Therefore, in Ti^{44}, the first particles outside the Ca^{40} core fill the ϕ_0 state, which is axial. The next four particles in Cr^{48} can go in either ϕ_{+1} or ϕ_{-1}, so in fact they occupy a linear combination of the two, leading to a triaxial solution. In Fe^{52}, both ϕ_{+1} and ϕ_{-1} are occupied and an axial solution is again possible. The next four particles can occupy the level ϕ_0', so Ni^{56} is axial. The calculated HF single-particle orbitals confirm this structure and fit the expected behavior exactly.

(*b*) *Finite spin-orbit force.* Table VI lists the results obtained with the infinite-range force and single-particle energies as given in Table I. The situation here is completely different than with zero spin orbit. The SU_3 scheme is very badly broken by the spin-orbit force, in contrast with the situation in the *s-d* shell. The spin-orbit force gives a large $f_{7/2}$-$f_{5/2}$ mixing up to four protons and four neutrons outside Ca^{40}. The $f_{7/2}$ level is only about 50% occupied. Beyond Cr^{48}, a considerable $p_{3/2}$ component is also present. But there is rather little f-p mixing, each orbit is either predominately $f_{7/2}+f_{5/2}$ or $p_{3/2}+p_{1/2}$. This indicates that it is not a very good approximation to consider $f_{7/2}$ as a separate shell, beyond Cr^{48}.

Beyond Fe^{54}, the infinite-range force is not very good because it does not bind the last occupied proton orbitals. It is probably just an indication that we have not really obtained the proper balance between the strength of the force and the spin-orbit splitting.

The finite-range results show rather less breaking of the SU_3 scheme. This may be another indication that the spin-orbit force is too strong in comparison to the strength of the infinite-range force. Calculations were also done for Ti^{44} using a variable spin-orbit strength. From the experimental energies (see Table I) the "center of mass" of the f and p levels were evaluated. Keeping the difference between the centroids $\epsilon_p-\epsilon_f$ ($=0.4$ MeV) constant, the strength α_{ls} was varied from the value 0 to -3.5. For $\alpha_{ls}=0$ there was a considerable mixing $f_{7/2}$ and $f_{5/2}$ (56% $f_{7/2}$ and 42% $f_{5/2}$) in the $k=\frac{1}{2}$ orbital, but it had very small ($\lesssim 2\%$) $p_{3/2}$ and $p_{1/2}$ components, i.e., as before there was no f-p mixing. As the strength was increased the $f_{7/2}$ component started increasing and for $\alpha_{ls}=-3.5$ the single-particle (s.p.) orbital $k=\frac{1}{2}$ had 92% $f_{7/2}$ and 7% $f_{5/2}$. It seems that independently of the strength α_{ls}, the infinite-range force breaks the SU_3 symmetry strongly.

IV. STABILITY OF THE HF SOLUTION IN Ti^{44}

The HF theory gives a purely independent-particle description of the nucleus.[16] In order to test the goodness of HF it is necessary to calculate the corrections to it due to correlation effects which have been neglected. These, for example, could be due to quadrupole vibrations or pairing effects. For the random-phase approximation[17] (RPA) they are described as particle-hole excitations on the HF state. We have tried to estimate these effects by doing RPA calculations on Ti^{44} ground state using schematic interactions.[17]

A. Quadrupole Vibrations

We assume that the residual interaction between particles moving in the self-consistent field is of the quadrupole-quadrupole type, viz.,

$$V_{ij}=-\chi\sum_{\mu} r_i^2 Y_{2\mu}(\sigma_i,\varphi_i) r_j^2 Y_{2\mu}^*(\sigma_j,\varphi_j),\tag{9}$$

where the coupling constant is approximately[18]

$$\chi\approx\alpha[2.9A^{-4/3}(h\nu)],\tag{10}$$

and α is a number which should be roughly equal to 2.[18] We will vary it (within reasonable limits) to see how our solutions are affected. $h\nu$ is the oscillator frequency. If we neglect the exchange terms in the interaction matrix elements, the RPA equations lead to the dis-

[16] One of us (J.C.P.) would like to thank Dr. D. J. Rowe for a number of useful discussions on the subject matter of this whole section.

[17] G. E. Brown, *Unified Theory of Nuclear Models and Forces* (North-Holland Publishing Co., Amsterdam, 1967).

[18] D. J. Rowe, Phys. Rev. **162**, 866 (1967).

persion equation[17]

$$\sum_{mi} \frac{|D_{mi}|^2(\epsilon_m-\epsilon_i)}{(\epsilon_m-\epsilon_i)^2-(\hbar\omega)^2}=(2\chi)^{-1}, \quad (11)$$

$$D_{mi}=(\sqrt{2})^{-1}\langle m|r^2[Y_{2\mu}+(-1)^{\mu}Y_{2-\mu}]|i\rangle. \quad (12)$$

Here m refers to a particle state (unoccupied HF orbital) and i to a hole state (occupied HF orbital). ϵ_m and ϵ_i are the HF s.p. energies of the states m and i, respectively, and $\hbar\omega$ is the energy of the collective vibrational state which we want to calculate. Using the HF results for Ti^{44} [see Table III(c)] and taking $\mu=0$ for β vibrations and $\mu=2$ for γ vibrations we get from Eq. (11) the following energies (in MeV) for different values of the parameter α (Table VII).

The energies for $\mu=0$ and $\mu=2$ lie at the top or above the HF gap, and so vibrations (quadrupole) should not be very important. Next, in order to get the ground-state [g.s.] correlated wave function we follow Sanderson[19] and Da Providência.[20] We get

$$|\mathrm{RPA}\rangle=N_0\exp\Big(\sum_{\alpha\beta} C_{\alpha\beta}\Gamma_\alpha^\dagger\Gamma_\beta^\dagger\Big)|\mathrm{HF}\rangle$$

$$=N_0\Big[1+\sum_{\alpha\beta} C_{\alpha\beta}\Gamma_\alpha^\dagger\Gamma_\beta^\dagger+\cdots\Big]|\mathrm{HF}\rangle, \quad (13)$$

where $\Gamma_\alpha^\dagger(\Gamma_\beta^\dagger)$ create a particle-hole pair when acting on the HF state, and boson commutation relations are assumed for these operators. N_0 is the normalization constant, and the coefficients $C_{\alpha\beta}$ give the correction to the HF wave function. They can be evaluated using an expression derived by Da Providência.[20] It turns out that the backward-going graphs make a negligible contribution, with the result that the correction to the HF wave function amounts to approximately 1%. Thus the nucleus seems to be very stable to quadrupole vibration effects since the wave function is so stiff.

B. Pairing Effects

Assuming that the nucleus does not make a superconducting transition we estimate the effect of the pairing interaction by calculating the energy and the correlated wave function for Ti^{44} including pairing vibration[21] effects. The residual interaction between particles moving in the HF field is taken to be

$$H_p=-G\sum_{\alpha\beta>0} a_\alpha^\dagger a_{\alpha-}^\dagger a_{\beta-}a_\beta. \quad (14)$$

α and β label the HF s.p. states (α_- is the time-reversed state of α). The coupling constant[21]

$$G=22/A. \quad (15)$$

[19] E. A. Sanderson, Phys. Letters **19**, 141 (1965).
[20] J. Da Providência, Phys. Letters **21**, 668 (1966).
[21] D. R. Bès and R. A. Broglia, Nucl. Phys. **80**, 289 (1966).

TABLE VIII. The $2p$-$2h$ amplitudes in the correlated ground state of Ti^{44}.

C_{21}	0.331
C_{31}	0.188
C_{41}	0.150
C_{51}	0.113
C_{61}	0.083
C_{71}	0.060
C_{81}	0.053
C_{91}	0.053
C_{101}	0.045

The dispersion equation and the expression for the RPA wave function are very similar to those for the quadrupole vibration. [For details we refer to the paper of Bès and Broglia (Ref. 21).]

Then the position of the lowest pairing vibration state in Ti^{44} is calculated to be at 1.4 MeV above the energy of the correlated g.s.—well within the HF energy gap. Further the g.s. wave function (normalized) is

$$|\mathrm{RPA}\rangle=\Big[0.752+\sum_{\omega\nu} C_{\omega\nu}\{(\Gamma_\omega^\dagger\Gamma_\nu)_p+(\Gamma_\omega^\dagger\Gamma_\nu)_n\}$$

$$+\sum_{\substack{\omega_1\nu_1\\ \omega_2\nu_2}} C_{\omega_1\nu_1}C_{\omega_2\nu_2}(\Gamma_{\omega_1}^\dagger\Gamma_{\nu_1})_p(\Gamma_{\omega_2}^\dagger\Gamma_{\nu_2})_n\Big]|\mathrm{HF}\rangle. \quad (16)$$

Here $\Gamma_\omega^\dagger=a_\omega^\dagger a_{\bar{\omega}}^\dagger$ and creates a pair of particles in an unoccupied HF state, while $\Gamma_\nu=a_{\nu-}a_\nu$ annihilates a pair of particles in an occupied HF orbital.[22] Labeling the HF orbitals from one to ten in order of increasing energy, we have in Ti^{44}, $\nu=1$ and $\omega=2,\cdots,10$. The coefficients $C_{\omega\nu}(\omega=2,\cdots,10,\ \nu=1)$ have the values shown in Table VIII.

Thus we see that the correlated g.s. is significantly modified from the HF state. Moreover, the intrinsic quadrupole moment of the RPA g.s. is reduced to 15.52 units from the HF value of 19.64 units. Therefore, the HF solutions are relatively unstable to pairing vibrations and their inclusion leads to an intrinsic state which is not as deformed as without them. In contrast to this, the pairing effects were very small in the $2s$-$1d$ shell.[23] In fact the corrections to the HF wave function would have been even larger if there was a possibility of having $4p$-$4h$ and higher terms in Eq. (16) for neutrons and protons.

Thus the reason why nuclei in $2s$-$1d$ shell show rotational features and those in $2p$-$1f$ shell do not seems to be the importance of pairing effects in the latter, in spite of the fact that in both the shells the HF wave functions have a reasonably pure SU_3 structure.

V. CONCLUSIONS

A remarkable similarity is seen in the nature of the HF solutions of even-even nuclei of the s-d shell and

[22] In Eq. (16) the subscripts p and n stand for protons and neutrons, respectively.
[23] M. K. Pal and A. P. Stamp, Nucl. Phys. **A99**, 228 (1967).

those in the p-f shell. These nuclei are found to be deformed, the deformation being prolate and increasing with the number of particles outside the core. There is a change in sign of the deformation for the heaviest nuclei studied here, the oblate solution becoming energetically more favorable than the prolate. Like in the s-d shell, the structure of the single-particle orbitals follows very closely the simple SU_3, or asymptotic Nilsson scheme. The spin-orbit force is not very effective in breaking the SU_3 symmetry. One significant difference from the s-d shell is due to the strong depression of the $f_{7/2}$ level by the spin-orbit force, leading to the closed-shell, spherical solution in Ca^{48}. Also the other calcium isotopes are, as a result, very nearly spherical, as seen by their small quadrupole moments and little mixing of single-particle orbitals of different j. However, in Ni^{56}, the eight neutrons and eight protons outside Ca^{40} do not completely fill the $f_{7/2}$ shell and the solution is not spherical.

On the other hand, the p-f-shell nuclei empirically do not show the characteristic deformed structure that is seen in the s-d shell. This we have seen is due to the most significant difference between the HF solutions in the p-f shell and those in the s-d shell. Namely, the gap between the occupied and unoccupied levels is smaller by about a factor of 3 in the p-f shell. Because of this, excitations across the gap occur much easier and effects of such particle-hole excitations become very important. In particular, the pairing correlations can change the structure of the excited states significantly from the simple rotational bands observed in the s-d shell.

This indicates that, although HF calculations in the p-f shell and heavier nuclei can be done and can yield interesting information about the structure of these nuclei, they are not in themselves adequate. Some sort of correlation must be allowed in the g.s. in order to account for the detailed structure of these heavier nuclei. It is therefore surprising that the structure of low-lying states of some nuclei in $2p$-$1f$ shell,[24] and even heavier ones like Mo and Nb isotopes,[25] can be reproduced by projecting states of good angular momentum from a single intrinsic determinant which is deformed, because this indicates an underlying single-particle picture of the nucleus.

ACKNOWLEDGMENTS

This work was started when the first author (J.C.P.) was at the Niels Bohr Institute in Copenhagen (Denmark). He would like to thank the Ford Foundation for a fellowship during this visit. We both extend our thanks to Professor Aage Bohr for his warm hospitality at the Niels Bohr Institute.

[24] K. H. Bhatt and J. C. Parikh, Nucl. Phys. **A98**, 113 (1967).
[25] K. H. Bhatt (private communication).

APPENDIX: INFINITE-RANGE-MODEL INTERACTION

The Yale-Shakin potential was replaced by a Gaussian, central potential with an arbitrary exchange mixture:

$$V(r)=V_0(W+MP_x+BP_\sigma-HP_\tau)\exp(-r^2/a^2). \quad \text{(A1)}$$

Here P_x, P_σ, P_τ are space, spin, and isospin exchange operators, respectively. Ideally, the parameters V_0, W, M, B, H, and a should be determined from a least-squares fit to the relative matrix elements $(nl|G|n'l')$ provided by Shakin *et al.*[6] However, this fitting should be weighted in some way since the relative matrix elements are not all equally important in any particular calculation; in particular, the smaller n values should have larger weights in the fitting than the large n. Since such a choice of weights is rather difficult and arbitrary, and since we only wanted the gross structure of the interaction, we decided to do a much simpler thing, namely to fit the diagonal, $n=0$ relative matrix elements of the $^1S_0$, $^3S_1$, $^1P_1$, and ^3P_J parts of the force exactly. Since there are no noncentral forces in (A1),the average ^3P state was fitted:

$$(0,{}^3\bar{P}|G|0,{}^3\bar{P}) = \sum_J (2J+1)(0,{}^3P_J|G|0,{}^3P_J)/\sum_J (2J+1). \quad \text{(A2)}$$

The value a was arbitrarily chosen as $a=1.68$ fm. Then we have four equations for the four parameters: W, M, B, H:

$$\begin{aligned} &W+M+B+H=1.0,\\ &W-M+B-H=-1.239,\\ &W+M-B-H=1.317,\\ &W-M-B+H=-0.0977. \end{aligned} \quad \text{(A3)}$$

The first of these is simply a normalization condition, and fixes V_0 in terms of the $^1S_0$ relative matrix element. The next three equations are the fits to the ^1P, ^3S, and $^3\bar{P}$ matrix elements, respectively. Solving these, we obtain $W=0.245$, $M=0.913$, $B=-0.365$, and $H=-0.206$. Also, $a=1.68$ fm and $V_0=-35.06$ MeV. To check these parameters, we calculated some of the higher-n matrix elements and found that they generally deviated by less than 10% from those given in Ref. 6. In addition, this exchange mixture was found to be quite insensitive to small changes in a.

When $a\to\infty$, the exponential factor in Eq. (A1) becomes 1 and we have the infinite-range model force we seek. V_0 should also change as $a\to\infty$. Its value is determined, therefore, to give a reasonable binding energy in Ti^{44}, as explained in the text. V_0 is unimportant for the zero spin-orbit work since then it is just an over-all factor, but it does matter for the finite spin-orbit results.